

# Final report for PD134579: Magnetic interactions and chemical disorder in complex magnets

Principal investigator: András Deák

## 1 Research background

We use the Screened Korringa–Kohn–Rostoker (SKKR) Green’s function technique to compute the electronic structure of crystalline systems. The method is designed to be performant and accurate for structures with only two-dimensional translation invariance (surfaces and interfaces), but it can also be applied to bulk systems. Thanks to a recent development we have made in our codebase, we now also have the option to treat bulk systems with “proper” three-dimensional Fourier transforms. We also have program suites building on top of our self-consistent calculations to extract classical spin models from the electronic structure, enabling multiscale approaches building from the *ab initio* level through atomistic spin simulations. The tensorial spin model we conventionally use is defined as

$$\mathcal{H} = -\frac{1}{2} \sum_{i \neq j} \mathbf{e}_i \underline{J}_{ij} \mathbf{e}_j + \sum_i \mathbf{e}_i \underline{K}_i \mathbf{e}_i, \quad (1)$$

where  $\mathbf{e}_i$  is a unit vector defining the orientation of the spin at site  $i$ ,  $\underline{K}_i$  is the on-site anisotropy matrix, and  $\underline{J}_{ij}$  is the Heisenberg exchange tensor comprising the isotropic Heisenberg interaction, the Dzyaloshinskii–Moriya (DM) interaction and the two-site anisotropy.

In the present final report we will list our research findings and the progress of the two-year research project.

## 2 Magnetization dynamics in high-anisotropy ferrimagnets

DyCo<sub>5</sub> is a member of a family of rare earth-cobalt ferrimagnets with some novel magnetic properties. In addition to its high magnetocrystalline anisotropy, there exists a temperature where the moment of the Dy and Co sublattices is compensated, which makes this material an excellent candidate for laser-induced magnetization switching applications, ultimately promising next-generation data storage devices. As the continuation of an earlier collaboration [1], we investigated the ultrafast demagnetization-remagnetization dynamics of DyCo<sub>5</sub> using a combination of femtosecond laser pump XMCD probe measurements and atomistic spin dynamics simulations based on *ab initio* model parameters. Our findings suggest that very different, element-specific damping parameters are necessary in order to explain the process, a trait which is likely applicable to a range of magnetic materials where different sublattices have vastly different spin-orbit coupling strength. The necessity of considering species-dependent damping parameters should especially be significant for the accurate description of ultrafast transient dynamics, such as ultrafast demagnetization, helicity-dependent all-optical switching and thermally induced magnetization reversal processes. Our results were detailed in Physica Status Solidi RRL [2].

## 3 Skyrmion lifetime in ferromagnet/heavy metal multilayers

We assessed the skyrmion life cycle using a multiscale description of an Ir/Co/Pt multilayer system, probing the stability of skyrmions and their thermal fluctuations. The isotropic Heisenberg interaction and Dzyaloshinskii–Moriya interaction strength from our calculations are shown in Fig. 1. The ground state of the system is a stripe domain phase, which can be understood as the result of sizeable antiferromagnetic Co-Co Heisenberg couplings

between the two Co interfaces destabilizing the ferromagnetic state, as well as significant DM interactions especially at the Co-Pt interface.

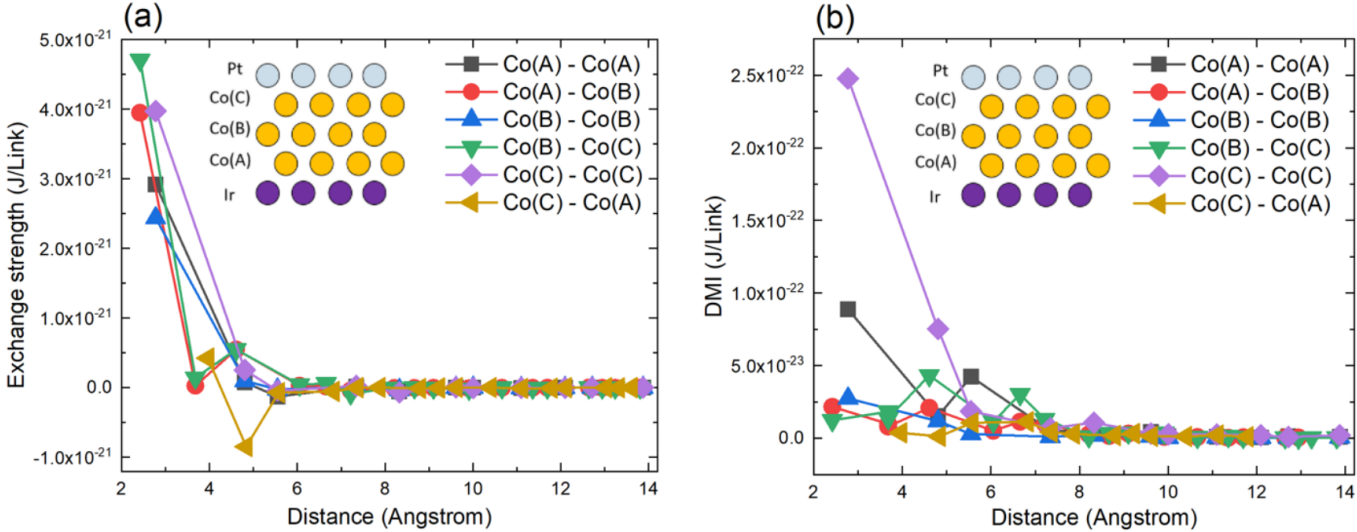


Figure 1: Isotropic Heisenberg exchange and Dzyaloshinskii–Moriya interaction strength in the Ir/Co/Pt interface system. Taken from Fig. S2 of the supplemental material of Ref. [3].

In addition to the existence of a hybrid phase where skyrmions and magnetic stripe patterns coexist, our simulations suggest that thermal creation and annihilation of individual skyrmions is possible at temperatures much lower than the Curie temperature. The gradually decreasing skyrmion lifetime and thermal creation/annihilation could lead to novel spintronics applications, for instance as thermal true random number generators. We published our results in Physical Review B [3].

## 4 Antiferromagnetic spintronics

### 4.1 Spin transport in hematite

Antiferromagnetic insulators have promising applications in the field of spintronics. Their very fast magnon dynamics (as compared to ferromagnons) and various spin transport effects hold the promise of high-speed, low-dissipation spintronics devices. We investigated the collinear antiferromagnetic insulator hematite ( $\alpha\text{-Fe}_2\text{O}_3$ ), focusing on its spin Seebeck effect, wherein a thermal gradient induces a magnonic spin current in the presence of an external magnetic field. We used a simplified atomistic spin model, combining parameters carefully fit to match static experimental quantities, and values distilled from *ab initio*-derived model parameters in order to obtain a qualitative description of the spin transport processes, supporting our collaboration’s experimental findings. We found transport of thermally excited magnon spin currents in the absence of a significant field induced magnetization parallel to the transport direction, with complex field-dependence of different magnonic contributions to the net transport signal. Our results published in Physical Review B highlight the importance of the Néel-order spin Seebeck conductance as a potential mechanism for tuning antiferromagnetic magnon transport in future applications [4].

### 4.2 Magnetic properties of hematite

Following our first results based on a simplified model of hematite [4], we carried on to provide a more complete description by making use of the full *ab initio* derived model for the material and its Morin transition [5]. Based on subsequent atomistic spin dynamics simulations, the computed tensorial exchange interactions result in a Néel temperature of 989 K and a weak ferromagnetic (WF) canting angle of  $0.038^\circ$ . The experimental values are about

950 K and  $0.06^\circ$ , respectively. The agreement in Néel temperature is excellent, and the about factor of two difference in WF canting angle has also been seen in earlier theoretical works, but its origin is unclear.

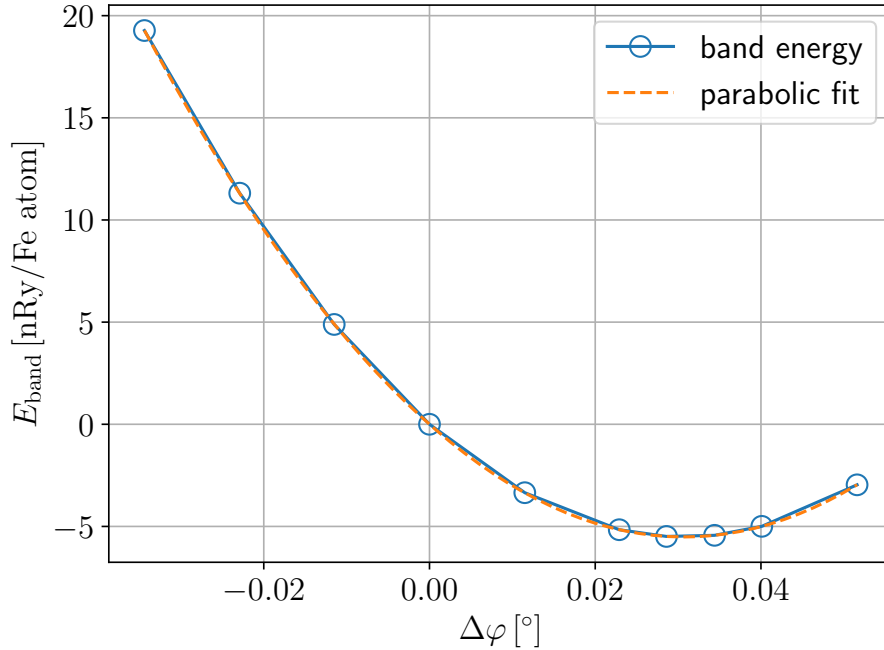


Figure 2: Energy of the weak ferromagnetic distortion in hematite relative to that of the in-plane AFM configuration. The two magnetic sublattices are oriented along an azimuthal angle of  $\Delta\varphi$  and  $180^\circ - \Delta\varphi$  with polar angle  $\vartheta = 90^\circ$ . The parabolic fit has minimum at  $\Delta\varphi_{\text{WF}} = 0.03071^\circ$  with 5.49 nRy/Fe atom energy difference.

The energy gain associated with the weak ferromagnetic distortion is only 5.5 nRy per Fe atom according to our *ab initio* calculations (cf. Fig. 2), which makes it clear that the WF distortion is not a driving mechanism, but rather a consequence of the Morin transition. In other words, the Morin transition is primarily a reorientation transition from out-of-plane antiferromagnetic (AFM) order to in-plane, driven by the competition of different anisotropy contributions, and once the spins are oriented in the plane, the DM interaction can enforce the WF distortion to further reduce the energy compared to the collinear in-plane AFM state. Our calculations also uncover the importance of the dipole-dipole interaction, which takes part in a subtle balancing act with the second and fourth order anisotropies to determine the ground state spin configuration.

We are currently in the process of reporting on our findings in a research paper, planned to be submitted in 2022.

### 4.3 Current-induced switching in $\text{Mn}_2\text{Au}$

We also investigated the switching dynamics of  $\text{Mn}_2\text{Au}$ , a key material for antiferromagnetic spintronics applications thanks to its property that the two magnetic sublattices transform into one another under inversion, enabling the emergence of electrically induced Néel spin-orbit torques. We combined *ab initio* calculated spin model parameters with susceptibilities describing electrically induced spin polarization (caused by the Rashba–Edelstein effect) computed from *ab initio* linear-response theory. We then used this combined model in atomistic spin dynamics simulations, investigating current-induced switching paths as well as corresponding timescales. Although from the spatial dependence of the isotropic couplings shown in Fig. 3 it is tempting to conclude that the three nearest neighbour shells dominate the interaction landscape, we find that neglecting further couplings significantly impacts the spin model.

Considering all interactions up to 2.7 lattice constant units we obtain effective spin model parameters in good agreement with both earlier theoretical works and experimental results. Of the switching dynamics we find that the

effect of electrically induced moments is insufficient for fully deterministic switching, and thus finite temperature is required in order to overcome the relevant energy barrier. We published our findings in Physical Review B [6].

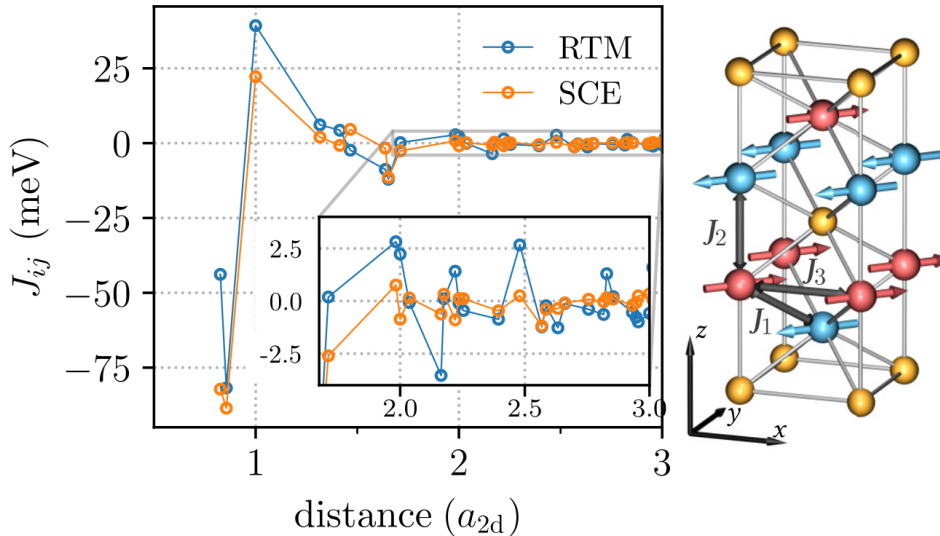


Figure 3: Isotropic Heisenberg couplings in  $\text{Mn}_2\text{Au}$  as a function of interatomic distance, and the first three nearest neighbours in the crystal. The dominant first two AFM and third nearest FM couplings are largely responsible for the ground state magnetic structure sketched in the right subfigure. “RTM” and “SCE” refer to the relativistic torque method and the spin-cluster expansion, respectively, two different methods we can use to extract a spin model from the electronic structure in a ferromagnetic and a paramagnetic reference state, respectively. Figure taken from Fig. 1 of Ref. [6].

## 5 Frustration-induced noncollinear magnetism

$\text{CrB}_2$  is a theoretically challenging example of an itinerant antiferromagnetic metal with incommensurate spin spiral ground state. We studied this material in terms of a spin model based on density functional theory calculations. We compare two methods (the SKKR, and the linearized muffin-tin orbital, or LMTO method), and two reference states (ferromagnetic order, and high spin temperature paramagnetic phase in the framework of the disordered local moment theory). We see overall good agreement between the two computational methods, especially in the paramagnetic state. Heisenberg exchange interactions derived from the paramagnetic phase using the disordered local moment theory show significant differences compared with those resulting from the treatment of the material as a ferromagnet; of these two methods, the disordered local moment theory is found to give a significantly more realistic description.

The isotropic Heisenberg interaction shown in Fig. 4 includes strong ferromagnetic couplings for the first two nearest neighbour shells, but numerous AFM further neighbour couplings give rise to such strong frustration that ultimately pushes the ground state away from ferromagnetic, and into a spin spiral state. Our calculations demonstrate that even in the paramagnetic state where the spin model parameters decay faster, it is necessary to include neighbours up to an interatomic distance of 2.8 lattice constant units in order to achieve convergence. With such a sufficiently converged model we find an ordering wave vector of magnitude  $0.213 \times (2\pi)/(a/2)$  along the  $\Gamma - \text{K}$  direction of the Brillouin zone, as opposed to the experimental value of  $0.285 \times (2\pi)/(a/2)$ . The Néel temperature of about 97 K we find is in good agreement with the experimental value of 88 K. Our underestimation of the wave vector is likely due to the strong frustration of the system, due to which very small changes to the spin model might tilt the energy landscape enough to lead to the emergence of a different ground state spin configuration. Since our model only includes bilinear interaction terms, it is plausible that higher-order multi-spin interaction terms, if included, would correct our ground state estimate.

Our work has been accepted for publication in Journal of Physics: Condensed Matter [7].

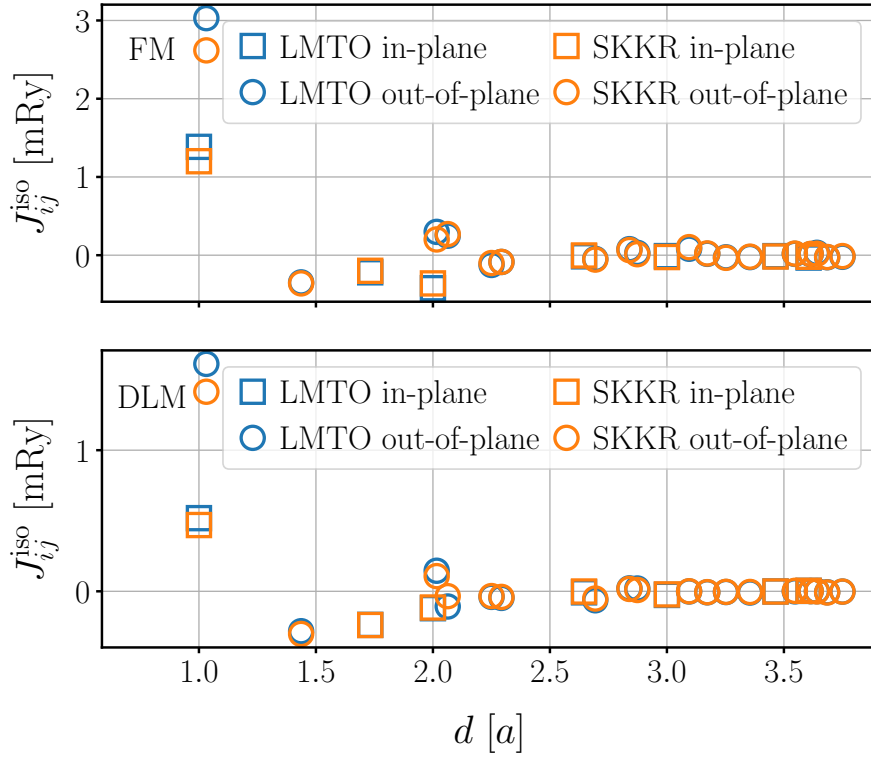


Figure 4: Isotropic Heisenberg couplings in  $\text{CrB}_2$  as a function of interatomic distance in units of the in-plane lattice constant. “SKKR” and “LMTO” refer to the two computational methods we used, whereas “FM” and “DLM” refer to the reference state considered for the corresponding calculations. Figure taken from Fig. 2 of Ref. [7].

## References

- [1] A. Donges, S. Khmelevskiy, **A. Deák**, R.-M. Abrudan, D. Schmitz, I. Radu, F. Radu, L. Szunyogh, U. Nowak, *Phys. Rev. B* **96**, 024412 (2017)
- [2] R. Abrudan, M. Hennecke, F. Radu, T. Kachel, K. Holldack, R. Mitzner, A. Donges, S. Khmelevskiy, **A. Deák**, L. Szunyogh, U. Nowak, S. Eisebitt, I. Radu, *Phys. Status Solidi RRL* **2021**, 2100047 (2021)
- [3] J. Wang, M. Strungaru, S. Ruta, A. Meo, Y. Zhou, **A. Deák**, L. Szunyogh, P.-I. Gavriloaea, R. Moreno, O. Chubykalo-Fesenko, J. Wu, Y. Xu, R. F. L. Evans, R. W. Chantrell, *Phys. Rev. B* **104**, 054420 (2021)
- [4] A. Ross, R. Lebrun, M. Evers, **A. Deák**, L. Szunyogh, U. Nowak, M. Kläui, *Phys. Rev. B* **103**, 224433 (2021)
- [5] F. J. Morin, *Phys. Rev.* **78**, 819 (1950)
- [6] S. Selzer, L. Salemi, **A. Deák**, E. Simon, L. Szunyogh, P. M. Oppeneer, U. Nowak, *Phys. Rev. B* **105**, 174416 (2022)
- [7] **A. Deák**, J. Jackson, B. Nyári, L. Szunyogh, *J. Phys.: Condens. Matter* (2022); accepted for publication, preprint available at arXiv:2209.11804